

# LIE MAP FORMALISM FOR FEL SIMULATION\*

Kilean Hwang<sup>†</sup>, Ji Qiang, Lawrence Berkeley National Laboratory, Berkeley, USA

## Abstract

Undulator averaging and non-averaging are in compromise between computational speed and reliability. It is hard to catch the advantages of the both methods simultaneously. In this report, we present a method that compromises the between the averaging and non-averaging methods through Lie map formalism.

## INTRODUCTION

In a more general sense, the method of averaging can be viewed by an instance of the re-formulation of the equations of particle and field motion to a numerically or analytically simpler form. Performance of such methods are based on analytic capability of producing accurate but simple enough equations and corresponding solutions that can alternatively describe the original system. A simple averaging can overlook the coupling between the betatron and wiggling motion, nonlinear and high order field strength. This coupling can be important when the undulator fringe field at entrance is not well tapered so that the averaged closed orbit is offset by half of the undulator oscillation amplitude. On the other hand, if one can obtain re-formulated equations that can describe the original system to a good accuracy, then it can have both advantages of averaging and non-averaging method. Such a robust set of equations can be derived using perturbative Lie map. Since the map over undulator period integrate out the fast undulator oscillation, the numerical performance can be as good as the method of averaging.

## OVERVIEW

To start with, we briefly review the perturbative Lie map method.

### Lie Map Perturbation

Let the Hamiltonian be decomposed with slow  $S$ , fast  $F$  and radiation field potential  $V$ , i.e.  $H(z) = S(z) + F(z) + V(z)$  where  $z$  is the longitudinal coordinate used as a time variable. Then, the map of the Hamiltonian system can be written by [1]

$$\mathcal{H}(z|z_0) = \mathcal{V}(z|z_0)\mathcal{F}(z|z_0)\mathcal{S}(z|z_0), \quad (1)$$

where  $z_0$  is the starting location of the integrator,  $\mathcal{S} \equiv e^{\mathcal{G}_S}$ ,  $\mathcal{F} \equiv e^{\mathcal{G}_F}$ ,  $\mathcal{V} \equiv e^{\mathcal{G}_V}$  are slow, fast, field map respectively,

and the generators of each map are

$$\begin{aligned} \mathcal{G}_S &= -\int_{z_0}^z dz : S : + \frac{1}{2} \int_{z_0}^z dz_1 \int_{z_0}^{z_1} dz_2 :: S_2 : S_1 : + \dots \\ \mathcal{G}_F &= -\int_{z_0}^z dz : F^{\text{int}} : + \frac{1}{2} \int_{z_0}^z dz_1 \int_{z_0}^{z_1} dz_2 :: F_2^{\text{int}} : F_1^{\text{int}} : + \dots \\ \mathcal{G}_V &= -\int_{z_0}^z dz : V^{\text{int}} : + \frac{1}{2} \int_{z_0}^z dz_1 \int_{z_0}^{z_1} dz_2 :: V_2^{\text{int}} : V_1^{\text{int}} : + \dots, \end{aligned} \quad (2)$$

where the interaction picture potentials are

$$\begin{aligned} F_i^{\text{int}} &\equiv \mathcal{S}(z_i|z_0)F(z_i) \\ V_i^{\text{int}} &\equiv \mathcal{F}(z_i|z_0)\mathcal{S}(z_i|z_0)V(z_i). \end{aligned} \quad (3)$$

### Field Model

In order to calculate the field map  $\mathcal{G}_V$  for particle motion, one need to know the force field priori. Therefore, the method we are presenting involves field modeling and requires the field solver to solve for the model field. This is a generalization of the spectral method. Since, we expect narrow-band and slowly varying envelope radiation, we model the radiation vector potential normalized by  $e/mc$  as

$$a_r \equiv \Re \sum_{h=1}^5 [\mathbb{K}_h + (z - z_0) \partial_z \mathbb{K}_h] e^{ih(\theta - k_u z)}, \quad (4)$$

where  $\theta = k_s(z - ct) + k_u z$  is the ponderomotive phase of radiation  $k_s$  and undulator  $k_u$  wave numbers.  $\mathbb{K}_h(x, y, \theta)$  is the model field envelope at each integration step. Note that dependence of field amplitude on  $z$  is removed while the longitudinal gradient  $\partial_z \mathbb{K}_h$  is included based on slowly varying envelope approximation. The gradient term and can be important for fast growth mode when the pre-unched beam is seeded [3], and thus can be beneficial for both averaging and non-averaging method. The order of magnitude of the normalized field strength is roughly about  $\mathbb{K}_1 \sim 10^{-6}$  at saturation estimated using  $P_{\text{rad}} \sim 1.6\rho P_{\text{beam}}$  and LCLS parameters [2].

### Effective Hamiltonian

In general, the solution of the perturbed map  $\mathcal{V}$  is not available, so it is hard to build a high order map out of the perturbed Lie map. On the other hand, an effective Hamiltonian can be obtained using Baker-Campbell-Hausdorff (BCH) formula.

$$\begin{aligned} H_{\text{eff}} &= -\frac{1}{L} (\mathcal{G}_S + \mathcal{G}_F + \mathcal{G}_V) \\ &\quad -\frac{1}{2L} (: \mathcal{G}_S : \mathcal{G}_F + : \mathcal{G}_S : \mathcal{G}_V + : \mathcal{G}_F : \mathcal{G}_V) + \dots \end{aligned} \quad (5)$$

Since the fast oscillating motion is already integrated out, re-concatenation of the perturbed Lie map through BCH formula can be well truncated within few orders.

\* Work supported by the Director of the Office of Science of the US Department of Energy under Contract no. DEAC02-05CH11231

<sup>†</sup> kilean@lbl.gov

## SLOW MAP

The normalized Hamiltonian for a particle in planar undulator is

$$H(x, p_x, y, p_y, \theta, \gamma/k_s; z) \quad (6)$$

$$= -\sqrt{\gamma^2 - 1 - (p_x - a_x)^2 - (p_y - a_y)^2} + (k_u + k_s) \frac{\gamma}{k_s},$$

where  $\gamma$  is the normalized energy, and  $a_{x,y} = eA_{x,y}/mc$  are normalized vector potentials. In a planar undulator the vector potentials are

$$a_x = K \cosh(k_x x) \cosh(k_y y) \cos(k_u z) + a_r$$

$$a_y = K \frac{k_x}{k_y} \sinh(k_x x) \sinh(k_y y) \cos(k_u z),$$

where  $K$  is the normalized undulator peak (not r.m.s.) strength and  $k_u^2 = k_x^2 + k_y^2$ . Here  $\cos(k_u z)$  is used instead of  $\sin(k_u z)$  assuming the undulator fringe field is tapered so that the averaged closed orbit is on-axis. We define the averaged Hamiltonian Eq. (6) as slow Hamiltonian,

$$S \equiv \frac{k_u}{k_s} \gamma + \frac{1}{2\gamma} \left[ 1 + p_x^2 + p_y^2 + \frac{K^2}{2} (1 + k_x^2 x^2 + k_y^2 y^2) \right]$$

$$+ \frac{K^2}{4\gamma} \left[ \frac{1}{3} (k_x^4 x^4 + k_y^4 y^4) + k_x^2 k_u^2 x^2 y^2 \right]$$

$$+ \frac{1}{(2\gamma)^3} \left( 1 + K^2 + \frac{3}{8} K^4 \right). \quad (7)$$

Note that  $\gamma^{-3}$  term is about same order of magnitude with the field potential when  $\mathbb{K}_1 \sim O(10^{-6})$  and  $\gamma \sim O(10^3)$ . We truncated Hamiltonian at  $O(10^{-12})$  assuming  $k_x x, k_y y, p_x, p_y \sim O(10^{-2})$  and  $\gamma \sim O(10^3)$ . Since the slow Hamiltonian is autonomous, the Lie map generator is simply

$$\mathcal{G}_S(L) = -SL. \quad (8)$$

## FAST MAP

We define the fast Hamiltonian by non-averaged part of the Hamiltonian independent of the radiation field, i.e.,  $F \equiv [H - S]_{\mathbb{K}_h=0}$ . After integrations, the generator of the fast map become

$$\mathcal{G}_F = -L \frac{K^3 k_x^2}{k_u^2 \gamma^3} \left( \frac{K}{16} - \frac{p_x}{3} \right) \quad (9)$$

where we assumed the initial location  $z_0$  and step size  $L$  are multiple of undulator period and included 3rd order of Magnus series not shown in Eq. (2). Although, it is as small as  $\gamma^{-3}$ , it is about same order of magnitude with radiation field potential when  $\mathbb{K}_1 \sim O(10^{-6})$  and  $\gamma \sim O(10^3)$ .

## FIELD MAP

The interaction picture potential of the radiation field for each harmonic  $h$  is

$$V^{\text{int}} = - \left( \frac{K_{\text{eff}}}{\gamma} \cos(k_u z) + \frac{p_x}{\gamma} \right) K_h^{\text{int}} \sum_{l,m}^{[-\infty, \infty]} J_l^{h\xi} J_m^{h\xi} e^{ih\psi_s^{\text{int}}}$$

$$\psi_s^{\text{int}} \equiv h\theta + h\dot{\theta}\delta z - (2l + m + h) k_u z$$

$$K_h^{\text{int}} = \mathbb{K}_h + \left( \frac{K_{\text{eff}}}{k_u \gamma} \sin(k_u z) + \frac{p_x}{\gamma} \delta z \right) \frac{\partial \mathbb{K}_h}{\partial x}$$

$$+ \frac{p_y}{\gamma} \delta z \frac{\partial \mathbb{K}_h}{\partial y} + \delta z \partial_z \mathbb{K}_h, \quad (10)$$

where  $J_n^a$  is the Bessel function of order  $n$  with argument  $a$ ,  $\delta z \equiv z - z_0$ , and

$$\dot{\theta} \equiv k_u - \frac{k_s}{2\gamma^2} \left( 1 + p_x^2 + p_y^2 + \frac{K_{\text{eff}}^2}{2} \right)$$

$$K_{\text{eff}} \equiv K \left( 1 + k_x^2 \frac{x^2}{2} + k_y^2 \frac{y^2}{2} \right).$$

Then, the Lie map generator can be written by the following form

$$\mathcal{G}_V = L \left( \frac{K_{\text{eff}}}{\gamma} \int_C + \frac{p_x}{\gamma} \int_0 \right) \mathbb{K}_h e^{ih\theta}$$

$$+ L \left[ \frac{K_{\text{eff}}^2}{k_u \gamma^2} \int_{SC} + \frac{K_{\text{eff}} p_x}{\gamma} \int_{1C} + \frac{1}{k_u} \int_S \right] \partial_x \mathbb{K}_h e^{ih\theta}$$

$$+ L \frac{K_{\text{eff}}}{\gamma} \int_{1C} \left( \frac{p_y}{\gamma} \partial_y \mathbb{K}_h + \partial_z \mathbb{K}_h \right) e^{ih\theta}, \quad (11)$$

where  $\int_i$  are integration parameters. Due to limited space in this paper, we write down few terms of the leading order integration parameter,

$$\int_C \equiv \frac{e^{-ih\theta}}{L} \int_0^L d(\delta z) \cos \psi_u e^{ih\psi_s^{\text{int}}}$$

$$= \frac{1}{2} \left( J_{-\frac{h+1}{2}}^{h\xi} + J_{\frac{1-h}{2}}^{h\xi} \right) + \frac{h\dot{\theta}}{4k_u} \left( J_{-\frac{h+1}{2}}^{h\xi} - J_{\frac{1-h}{2}}^{h\xi} \right)$$

$$+ \sum_{l \neq -\frac{h+1}{2}, \frac{1-h}{2}} \frac{h\dot{\theta}}{k_u} \frac{(2l+h) J_l^{h\xi R}}{(2l+h+1)(2l+h-1)}$$

$$+ \dots \quad (12)$$

The first term is so-called coupling factor. Although  $\dot{\theta}/k_u$  is small due to resonance condition, it is as important as the coupling factor contribution on  $d\theta/dz$  as can be seen from Eq. (13)

$$-\frac{\partial \mathcal{G}_V}{\partial \gamma} \propto \frac{1}{2\gamma^2} \left( J_{-\frac{h+1}{2}}^{h\xi} + J_{\frac{1-h}{2}}^{h\xi} \right) - \frac{hk_s}{4\gamma^4 k_u} \left( J_{-\frac{h+1}{2}}^{h\xi} - J_{\frac{1-h}{2}}^{h\xi} \right) + \dots \quad (13)$$

## COMPARISON

Here, we present comparison between our method and GENESIS pusher [4]. We take the particle tracking using

original Hamiltonian Eq. (6) with small enough time step to represent exact solution. In order to compare the particle pusher independent of the field solver, the radiation field is modeled by transversely Gaussian envelope of rms size same with the electron beam. Undulator parameters used are  $K = 1.5$ ,  $k_x = k_y = k_u/\sqrt{2}$ ,  $\lambda_u = 2.5$  cm. We prepare initially matched Gaussian electron beam truncated at  $3\sigma$  with normalized emittance  $1\mu\text{m}$  and  $\sigma_\gamma/\gamma = 0.01$ . In order to quantify the error, we use  $|\theta - \theta_{\text{exact}}|/2\pi$  and record the error for each particles. Integration step size is chosen by one undulator period at which the numerical error due to large step size showed convergence. In other words, the error shown in figures originates from the inaccuracy of the re-formulated equations by averaging or Lie map method. Figure 1 shows the error in the absence of the radiation field showing an order of magnitude better accuracy. Figure 2 shows the error under radiation field whose normalized strength is  $\mathbb{K} = 10^{-6}$  which corresponds to the field strength near saturation in case of LCLS. Figure 3 shows the error under exponentially growing radiation field with growth rate  $L_G \sim 10^2 \lambda_u$  and initial strength  $\mathbb{K} = 10^{-8}$ . Inclusion longitudinal field gradient in Eq. (10), made the accuracy as good as the zero radiation case of Fig. 1. This can be especially important when much shorter gain length  $< 10^2 \lambda_u$  is achieved.

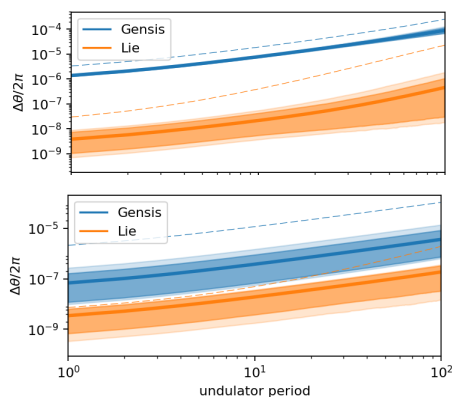


Figure 1: Ponderomotive phase error in the absence of the radiation field. Top and bottom corresponds to  $\gamma = 10^3$  and  $\gamma = 10^4$  respectively. Thick line represent the average, shadowed area corresponds to the error of 90% and 95% population for lighter and darker shade. The dashed line corresponds to the maximum error.

## CONCLUSION

A compromised method between averaging and non-averaging method is presented and tested. More robust equations of motion than undulator averaging is derived using perturbative Lie map. Simulation result shows good improvement on the accuracy while the computation time was only about 1.3 times of the method of averaging. In order to build a Lie map, we had to model the radiation field. The modeled field ansatz is what we need to solve in field solver which is our next research plan.

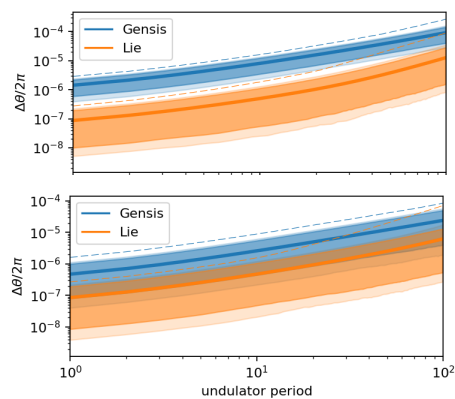


Figure 2: Ponderomotive phase error at radiation field strength  $\mathbb{K} = 10^{-6}$ . Top and bottom corresponds to  $\gamma = 10^3$  and  $\gamma = 10^4$  respectively.

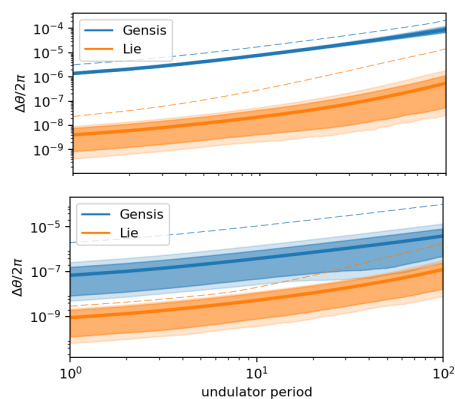


Figure 3: Ponderomotive phase error at initial radiation field strength  $\mathbb{K} = 10^{-8}$  and exponentially growing by rate  $L_G \sim 10^2 \lambda_u$ . Top and bottom corresponds to  $\gamma = 10^3$  and  $\gamma = 10^4$  respectively.

## ACKNOWLEDGEMENT

We appreciate valuable discussion with Gregory Penn. This work is supported by the Director of the Office of Science of the US Department of Energy under Contract no. DEAC02-05CH11231

## REFERENCE

- [1] A. Dragt, "Lie Methods for Nonlinear Dynamics", <http://www.physics.umd.edu/dsat>
- [2] [https://portal.slac.stanford.edu/sites/lclscore\\_public/Accelerator\\_Physics\\_Published\\_Documents/LCLS-parameters-3-22-17.pdf](https://portal.slac.stanford.edu/sites/lclscore_public/Accelerator_Physics_Published_Documents/LCLS-parameters-3-22-17.pdf)
- [3] L. H. Yu., "Generation of intense uv radiation by subharmonically seeded single-pass free-electron lasers", *Phys. Rev. A*, vol. 44, p. 5178–5193, 1991.
- [4] S. Reiche, "GENESIS 1.3: A fully 3D time-dependent FEL simulation code", *Nucl. Instrum. Methods Phys. Res., Sect. A*, vol. 429, p. 243, 1999.